Journal of Environment and Earth Science www.iiste.org
ISSN 2224-3216 (Paper) ISSN 2225-0948 (Online)
Vol.6, No.12, 2016

Simulation of Regional Groundwater Flow in Semi-Arid Farm

Sagarika Roy[1,2*] Duke Ophori[2]
1.Undergraduate Program, Indian Institute of Science, Bangalore, India
2.Earth and Environmental Studies, Montclair State University, New Jersey, USA

Abstract
A mathematical groundwater flow model is developed for drought affected semi-arid farm located in southern San Joaquin Valley, California. The objective was to simulate the flow direction and capture the potential recharge areas for water stressed crops. A finite difference grid of 20 rows and 35 columns was spaced with 700 active cells in X and Y directions and five layers in Z direction. The boundary conditions were selected from the USGS topographic map. MODFLOW-2000 integrated in Groundwater Modeling Software (GMS) was used to simulate 3-D flow. There are five observational wells in the study area monitored by California Water Science Center (CAWSC) and California Department of Water Resources (DWR). Available meteorological, geological and hydro-geological data were used to characterize the existing groundwater conditions and to simulate the equi-potential surface. The model was calibrated using groundwater elevation data against the historical water level data under steady-state conditions. A transient simulation was carried out from the year 2006 to 2011 for 5 stress periods. Results showed that the groundwater flows from west to east of the study area towards the California Aquaduct causing the drop in water table in the wells at the study area. The average water surface elevation (WSE) in 1950 for the growing season (May to July) was 161.04 m. This value is low when compared to those of 2009, 2010, and 2011, which are 237.14, 236.28, and 235.74 m respectively.
Keywords. MODFLOW, GMS, finite difference, hydrogeology, modeling, recharge.

1. Introduction

The impact of drought in California is a major concern that is affecting the agricultural and farming production in the Central Valley. The years 2006-11 were the 12th consecutive 5-year drought-period in recorded climatic history based on precipitation index (California Department of Water Resources, 2009). It is estimated that poor rainfall and over-exploitation of water resources hampered both the agricultural productivity and water reservoir levels. It is studied that the State had agricultural losses of $ 308 million in 2008 from lack of water resulting in high crop prices (California Department of Food and Agriculture, 2009). Understanding groundwater dynamics is of primary importance in water resources planning and management in extensively irrigated fields. Mining groundwater for agriculture and domestic purposes has lead to the depletion of natural resources. In southern San Joaquin Valley, California, an intensive exploitation of groundwater for domestic and irrigation supply exists to offer abundant irrigation to one of the most productive agricultural districts. "About one-fifth of the groundwater discharge is from the Central Valley aquifer system, and as a result, the groundwater in southern San Joaquin Valley is below drought period water level" (Roy et al., 2012). It has Mediterranean climate, with hot and dry summer and wet winter. It rains in winter months (December to February) and remains arid during the growing season of orchards (May to July). Therefore, the optimal use of limited groundwater resources in this region is of primary importance. The study area is located in the Central Valley aquifer system in California. This study area was selected because almond orchards are the only commercial crop grown in San Joaquin valley in California and it is world largest supplier of almond. These orchards are a long-term investment and need specific irrigation scheduling. However, they can provide excellent returns to growers over a prolonged period. In addition, these crops are sensitive to over-irrigation, which can result in hull-rot disease (Roy et al, 2012). The water delivery for the Central Valley Project (CVP) reduced to 10 percent of contractor's allocations to be used for irrigation in 2009 compared to 40 percent in 2008 and 50 percent in 2007 (California Department of Water Resources, 2009). This is a very critical situation as CVP followed stringent rules for water allocation for farms every year; therefore, mining of groundwater is only alternative for farmers to accommodate the water shortage. The groundwater abstraction in California is known to be the second largest withdrawal of United States (Maupin, 2005). Under pre-development condition (prior to development of surface water diversions), the total recharge and discharge was observed to be under steady state (Bertoldi et al., 1991; Willliamson et al., 1989). Williamson et al., (1989) suggested that due to the population growth in late 1900, and massive agricultural water demand, the estimated recharge and discharge observed was 16.4×10^9 and 18.1×10^9 m^3/yr respectively and the change in the storage is -1.7×10^9 m^3/yr (Willliamson et al., 1989). The natural pattern of groundwater flow and the rate of recharge-discharge were significantly altered by pumping, and by surface water diversion for irrigation especially during drought periods.

Groundwater withdrawal from wells has lowered the water table and altered the flow direction, causing land subsidence and change in groundwater flow pattern (Willliamson et al., 1989). Williamson (1989) computed the groundwater flow and storage between 1920 and 1950 and suggested that many locations in the San Joaquin Valley, the groundwater level declined between 12 and 25 meters. Study shows that between 1920 and 1950, groundwater level declined significantly from the expansion of agriculture as a result, irrigation was depended mainly on groundwater in many parts of San Joaquin Valley (Willliamson et al., 1989). However, since 1950 to 1955, the development of CVP, and Friant – Kern Canal that distributed the surface water to many parts of San Joaquin Valley has significant effect on the groundwater table. This resulted in decrease in groundwater pumping causing the water-table to raise in San Joaquin Valley (Faunt et al., 2009; Willliamson et al., 1989).

The hypothesis is tested for this study area to understand the increase of groundwater level since 1950, because irrigation is more dependent on surface water diversion from the San Joaquin River and California Aquaduct. Hence, loss of irrigation water to percolation could be the reason for ground-water level to rise in the study area. The objective of this study are (1) to simulate three dimensional groundwater flows in the entire study, (2) to capture the potential zones of recharge, and (3) to compare the Water Surface Elevation (WSE) between historic data and 2009 to 2011.

2. Materials and Methods

2.1. Study area

The 402 km^2 farm is located at Kern County in southern part of San Joaquin Valley of Central Valley, California (35^{o}30'N, 119^{o}39'W) (Figure 1). The valley is the most productive region for agriculture occupying most of the southern Central Valley, California. The study area is most dominated with almond orchard farm comprises two third of the southern part of the Valley. This area is geographically situated between Sierra Nevada on the east and the Coast Ranges on the west , the southern part of the San Joaquin Valley is the Tulare Basin, bordered the Tehachapi Mountains on the south. The northern extent corresponds to the Kings River. The valley comprises of arid to semi-arid climatic condition with an annual rainfall of 98.5 mm. San Joaquin River flows from Sierra Navada in the east, flowing across the valley and drains in the Sacramento-San Joaquin delta in the North. Most of the stream-flow from Kings and Kerns rivers flows from east towards Sierra Navada in the west.

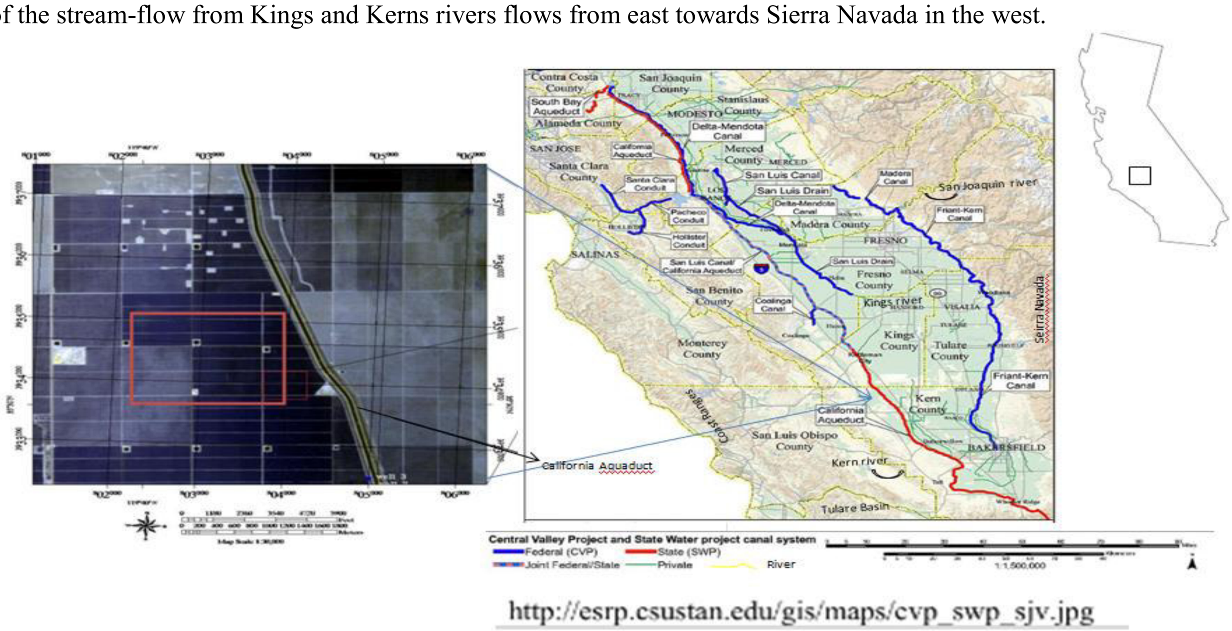

Figure 1. Study area (red box) showing the location of the farm in Southern San Joaquin Valley, California (left). Blocks in dark tone shows various types of crops. Bright tone shows non-vegetated/arid areas. Right Inset: Map of Southern Joaquin Valley with Central Valley Project canals (blue lines), State Water Project (red lines) and rivers (yellow lines). Top inset: Map of California.

2.2. Regional Hydrogeology

Figure 2 shows the regional hydrogeology of the study area derived from the large, northwest trending asymmetric structural trough which comprises marine and continental sediments up to 10 km thick (Gronberg et al., 1998; U.S Bureau of Reclamation, 2009). These sediments are significantly deposited largely by streams draining from the mountains from time to time. The alluvial fan in this area is derived from the glaciated portion of the Sierra Nevada (Faunt et al., 2009). Fine-grained sediments (clay, sandy clay, sandy silt, and silt) are distributed throughout the San Joaquin Valley (Bertoldi et al., 1991; Faunt et al., 2009). The distribution of upper Miocene sand known as Stevens Sand (Bazeley, 1972) in late Miocene occurring in southern San Joaquin Valley comprises discontinuous sand bodies separated by thin shale interbeds (Webb, 1977)

The Corcoran Clay forms a separation in the basin-fill deposits into an upper unconfined to semi-confined zone and a lower confined zone in southern San Joaquin Valley (Willliamson et al., 1989; Mendenhall et al., 1916). The Sierra Nevada rises to an elevation of more than 4200 m in the east of the valley; whereas, west of the valley area is bounded by the Coast Ranges which are a series of parallel ridges with moderate elevations (Mendenhall et al., 1916; U.S Bureau of Reclamation, 2009).

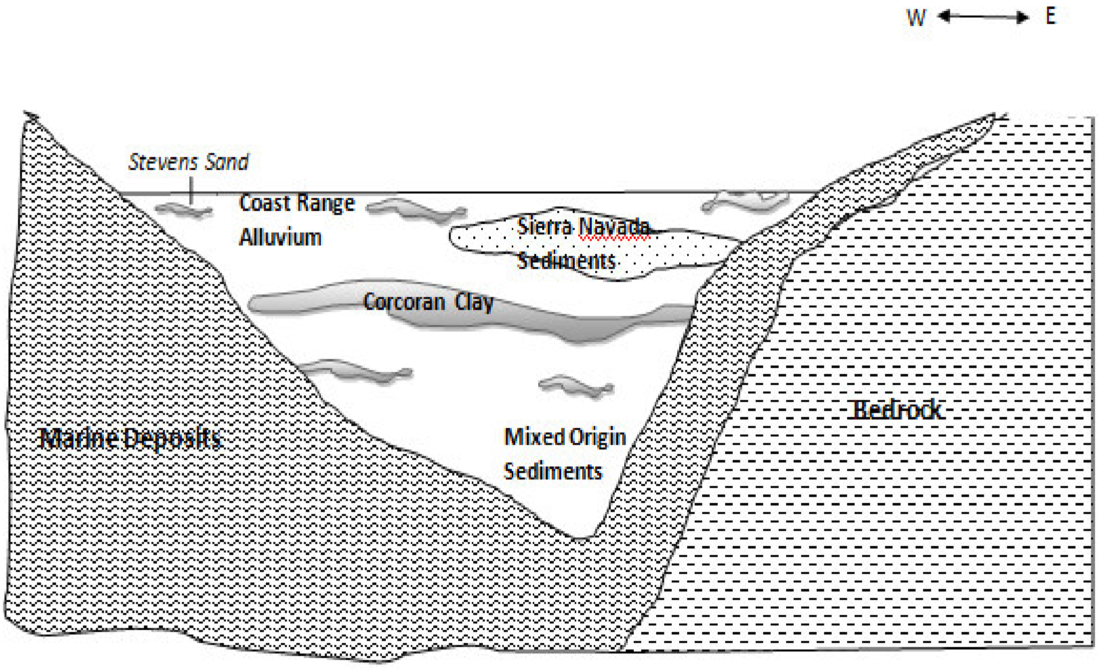

Figure 2. Cross section representation of regional hydrogeology of the study area
Source: Reclamation et al. 1990 (U.S Bereau of Reclamation 2009)

2.3 Available Data

The base map of the study area was developed from a topographic map of scale 1: 250000 acquired from the United States Geological Survey (USGS) website. Soil texture and soil moisture capacity of the study area is shown in the Table 1 (Ratlliff et al., 1983). The elevation model constructed from the USGS topographic map. The land-use/land cover map is produced from the remote sensing image acquired from MASTER (MODIS/ASTER) sensor onboard the aircraft NASA-DC-8. It shows that about 80% of the land is under agriculture and less than 10% is urban (Figure 3) (Roy et al., 2013).

The litho-stratigraphic data was acquired from geophysical electric log in 1978. Five observation wells in the study area monitored by USGS California Water Science Center (CAWSC) and California Department of Water Resources (DWR) (California Department of Water Resources, 2009). Water Surface Elevation (WSE) data for 1950 and 2009 to 2011 is obtained from DWR website. Meteorological data is available from California Irrigation Management Information System located in Belridge. Meteorological and hydrological data are used as input data to characterize the groundwater conditions in this aquifer and to simulate potential recharge and discharge scenario.

Table 1. Soil moisture capacity of the Paramount Farm (Ratliff et al., 1983)

Soil texture	Available water capacity (mm per meter of thickness)	Maximum soil water capacity (mm)
Sand	14400	182.88
Loamy Sand	22800	289.56
Sandy Loam	30000	381
Loam	38400	487.68
Silt loam	43200	548.64
Sandy clay Loam	42000	533.4
Sandy clay	40800	518.16
Clay loam	45600	579.12
Silty clay loam	51600	655.32
Silty clay	57600	731.52
Clay	4.8	28.8

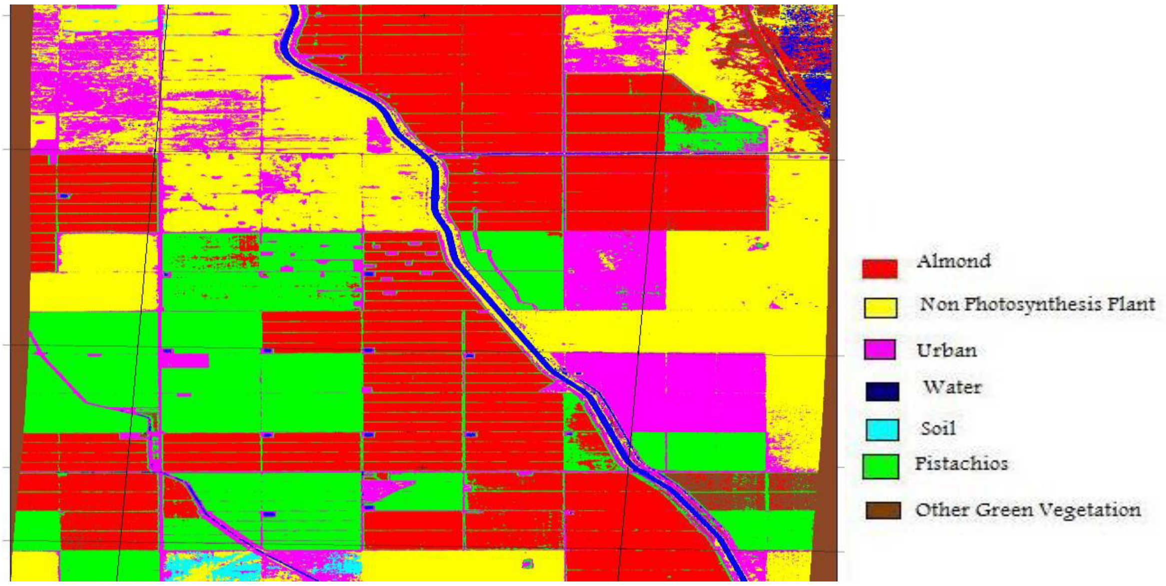

Figure 3. Land Use and Land Cover Classification. (Roy et al., 2013)

2.4. Hydrologic framework and conceptualization

The conceptual model of the study area was done by selecting a domain of 24000 m by 17000 m in X and Y directions respectively (Figure 4). The Z dimension comprises five litho-stratigraphic layers derived from borehole log data. The aquifer is divided into 5 layers based on sub-surface lithology. The first layer is unconfined, 400 m thick and comprises sand followed by sandy loam, silt loam, sandy clay and clay in layers 2, 3, 4, and 5 respectively. The second, third and fourth layers were assumed to be 100 m, 50 m, 25 m thick respectively. Based on well logs data the aquifer parameters were specified accordingly (Table 2). The borehole log data obtained by Shell oil Co. at the location in Elk Hills were used to know the aquifer properties. The available data show that the hydraulic conductivity ranges between 0.0008 to 100 m/day. Storage coefficients for layer 1, 2 and 3 are 1.8×10^{-3}, 1.1×10^{-3} and 4.5×10^{-3} m^{-1} respectively whereas for layer 4 and 5 ranging from Sandy clay to Clay are 8.5×10^{-6} and 2.3×10^{-6} m^{-1}, respectively. The top boundary was assigned by specifying a hydraulic head value at each node denoted as constant head (Berry et al., 2009; Ophori et al., (1989). The bottom boundary is a confining boundary represented by the Corcoran clay. To understand the complexity of the system, several assumptions are made to simplify modeling approach. Generally, it is known that the surface-water divide coincide with ground-water flow divide (Berry et al., 2009; Ophori et al., 1989). Therefore, California Aqueduct bounds the eastern side of the study area that was considered a no-flow boundary. Also, hills are assumed to be groundwater flow divide due to its topographically high areas. On the west of the study area is Elk hills, assumed to be a no-flow boundary. The north and south of the area bounded by Emigrant Hill and West Elk Hill respectively are considered as no-flow boundary. The observation wells were monitored for water surface elevation in the study area are shown in Table 3.

Table 2. Aquifer parameters

Model Layer	Top Elevation (m)	Bottom Elevation (m)	Litho-stratigraphy of layers	Hydraulic Conductivity (m/day)	Vertical Anisotropy
1	600	200	Top soil: Stevens Sand	100	6
2	200	100	Sandy Loam	0.15	3
3	100	50	Silt Loam	0.018	3
4	50	25	Sandy clay	0.001	3
5	25	0	Clay	0.0008	3

Table 3. Description of observational wells in the locations monitored by DWR

Wells	Well site number	Location of the wells (coordinates)	XY grid cell	Ground Surface Elevation (m)	Water surface Elevation (m) msl	Depth to the water (m)
1	28S22E18C002M	35.49N, 119.64W	14,29	302	268.1	28.7
2	28S22E08D002M	35.51N, 119.63W	15,30	258.29	249.16	15.9
3	26S21E27P061	35.63N, 119.66W	7,28	233.8	221.6	13.1
4	26S21E27R061	35.63N, 119.69W	5,27	242.5	231.2	11.6
5	28S22E05F002M	35.52N, 119.63W	6,28	235.7	222.4	15.3

2.5. Numerical Model:

The next step in modeling is converting the conceptual design into a numerical model. A three dimension groundwater flow simulation is developed to model the regional flow pattern in the study area. The finite difference method uses a numerical solution for the following groundwater flow equation for three-dimensional saturated flow in saturated porous media:

$$\frac{\partial}{\partial x}\left(Kxx\frac{\partial h}{\partial x}\right)+\frac{\partial}{\partial y}\left(Kyy\frac{\partial h}{\partial y}\right)+\frac{\partial}{\partial z}\left(Kzz\frac{\partial h}{\partial z}\right)-Q=Ss\frac{\partial h}{\partial t} \quad (1)$$

where *Kxx, Kyy, Kzz* are hydraulic conductivity along the x, y, z axes which are assumed to be parallel to the major axes of hydraulic conductivity (L/T);
h = hydraulic head (L);
Q = volumetric flux per unit volume representing source/sink terms (1/T)
Ss = specific storage defined as the volume of water released from storage per unit change in head per unit volume of porous material (1/L).
t = Time (T)

The equation that describes three-dimensional steady-state groundwater movements through porous earth material under equilibrium condition is given by the partial differential equation

$$\frac{\partial}{\partial x}\left(Kxx\frac{\partial h}{\partial x}\right)+\frac{\partial}{\partial y}\left(Kyy\frac{\partial h}{\partial y}\right)+\frac{\partial}{\partial z}\left(Kzz\frac{\partial h}{\partial z}\right)=0 \quad (2)$$

The finite difference code, MODFLOW in the GMS package was developed by [McDonald et al, 1998, 1996a) is used to simulate groundwater flow pattern and capture the recharge areas of the study area. The conceptual model was numerically converted into finite-difference grids. The grid consists of 20 rows and 35 columns with 700 active cells in X and Y directions, respectively. The cell size is 100 m by 100 m. The model was divided vertically into 5 layers of variable thickness that extend from the top soil to the basement shown in Table 2 and Figure 4.

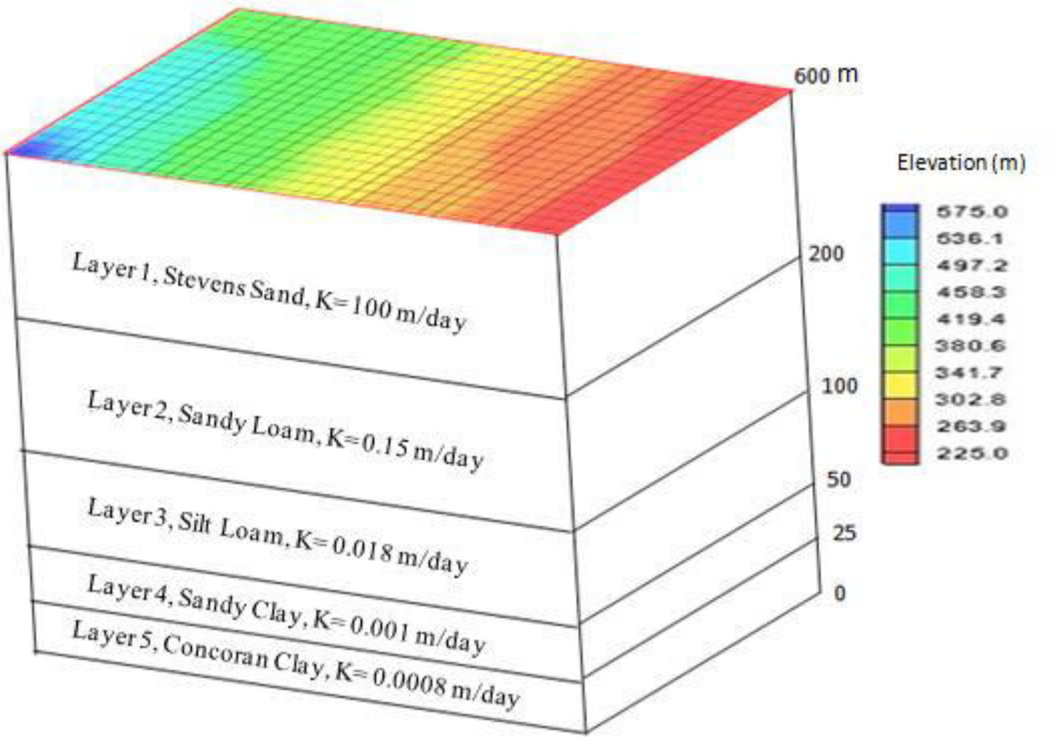

Figure 4. Conceptual framework of hydrostratigraphic units in the study area used for constructing digital model.

3. Result and Discussion

Initially, homogeneous and isotropic conditions were assumed throughout the basin to analyze the steady state condition. The numerical model was developed from the piezometric data. With the hydraulic head distributed in the first layer, the mathematical finite difference model was generated in each node to determine the equipotential lines in the surface and study the flow distribution of groundwater in the area. The flow vectors are perpendicular to the equipotential lines and thus show the direction of groundwater at every point in the flow domain. After every simulation, calculated hydraulic head were compared with observed hydraulic head. Referring the Table 2 and 3 simulated hydraulic head was produced by changing hydraulic conductivities as necessary using the values ranging from Stevens sand (100 m/d), Sandy Loam (0.15 m/d), Silt Loam (1.8×10^{-2} m/d) to Concoran clay (8×10^{-4} m/d) to distinguish the aquifers from the aquitard which is necessary to simulate anisotropic conditions. Best match between observed and simulated hydraulic head distribution produced from Table 3 is generated and the resulting hydraulic head distribution is shown in Figure 5a. The final calibrated hydraulic conductivity values for model layer 1-3 were 15 , 0.11 and 0.011 m/d respectively. The flow arrows indicate that the groundwater flow direction is from west to east in the study area. It is moving towards the California Aqueduct.. It was observed that the highest hydraulic head in the entire model area is located in the southwest side of the area.

(a)

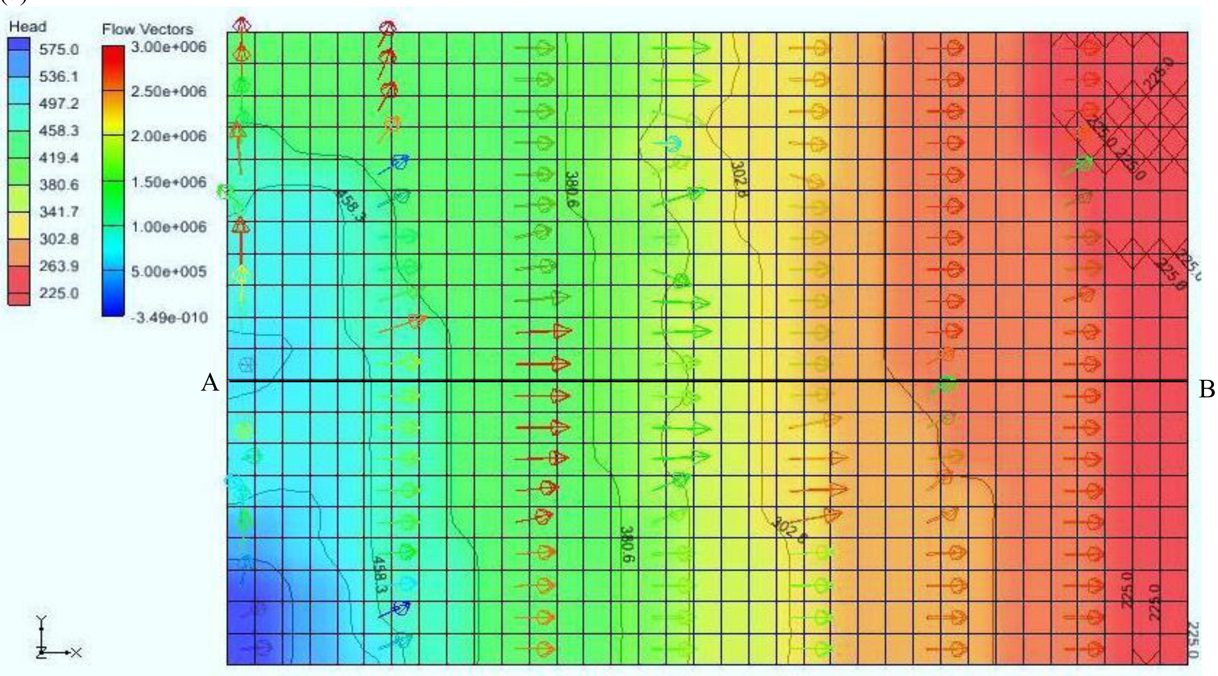

(b)

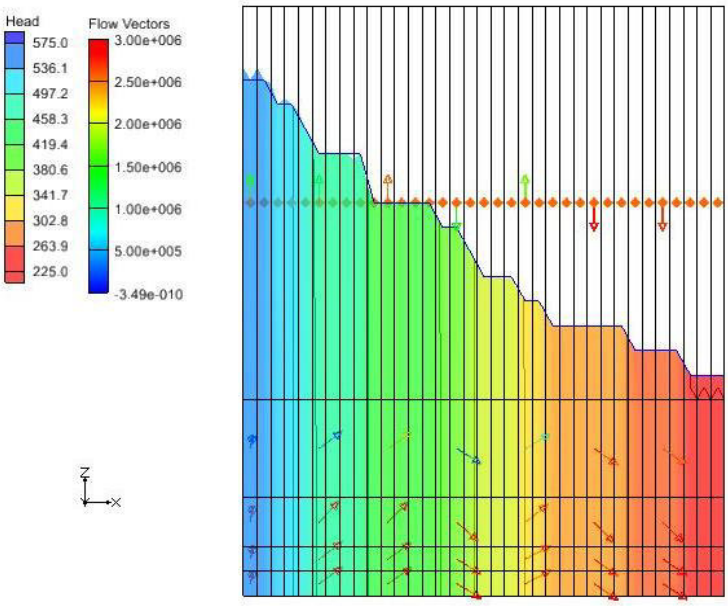

Figure 5 (a). Showing horizontal cross section of piezometric surface map (Z axis) based on the steady state simulation model. **5(b)**. Groundwater flowing in vertical cross-section in X and Y axis to analyze the recharge and discharge nodes. Orange dot indicates ground surface.

The computed recharge-discharge shown in Figure 5b indicates a series of groundwater flow into and out from the different layers of the aquifer. The discharge shown with upward arrows are those nodes where there is drawdown of groundwater. The downward arrows show the recharge of water from the agricultural areas. Therefore, the irrigated water, which is mostly percolated from the well-irrigated region of the farm, is flowing towards the California Aqueduct. Hence, in future studies, the subsurface artificial recharge structure such as percolation tank, infiltration gallery, and subsurface barriers will be proposed in the potential area of recharge (Figure 6) to minimize the outflow of groundwater from the study area during drought period.

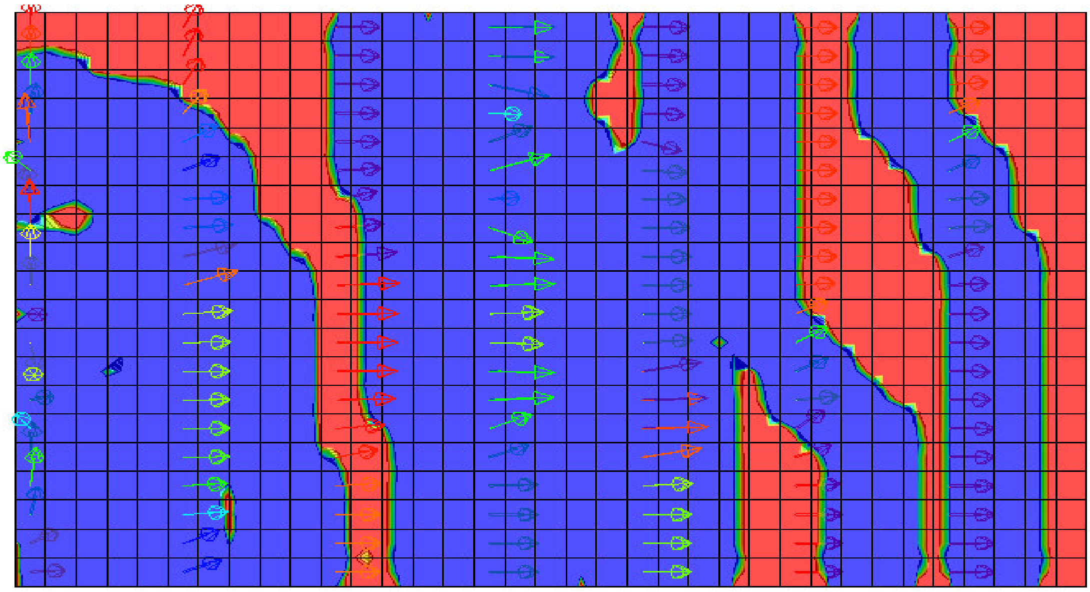

Figure 6. The potential areas of recharge in red indicating the percolation and movement of water in the lower horizontal layer of the model

In order to assess the potential zone of recharge (Figure 6), the domain is characterized by various infiltration rates of different soil type with variation in groundwater pumping in the study area. Recharge and discharge can be analyzed quantitatively to determine the total groundwater discharge through the system. The models estimated a total discharge that is equal to recharge assuming steady state of 1.58 x 10^{-5} m^3/s. Steady-state conditions were calibrated using water levels in 5 wells in the area. [15] stated that "the water table is commonly a subdued replica of the surface topography" and calibrated steady-state model to the land surface elevation (Ophori et al., 1989; Berry et al., 2009). In model calibration, data from the five wells were taken for the year 2009 to represent the period of drought with maximum pumping of wells for reasonable period in the study area. The observed versus simulated water level plotted on a graph to understand the good match. The relation between observed and simulated water levels in wells (Figure 8) suggested that the simulated water level is close with observed water level with regression coefficient of 0.78 are acceptable for the model .

The transient simulation was carried out from the year 2006 to 2011 for 5 stress periods occurred due to drought (Eq. 1). Groundwater withdrawal had several effects in the study area causing significant water level fluctuations and drop in the water table. Figure 7 shows the distribution of hydraulic heads and its drawdown at the end of first stress period. It is observed that due to groundwater pumping during drought period, the water table is declined and flowing away from the wells (Figure 7). Under such conditions, where the groundwater was heavily pumped, the groundwater flows beneath the surface water (rivers/streams) instead of discharging into the surface bodies. In order to estimate the transient effect, the pumping wells will have the potential to capture water from recharge areas and this will reduce discharge and shortage (Berry et al., 2009) and therefore, the potential area of surface water infiltration is shown in Figure 6.

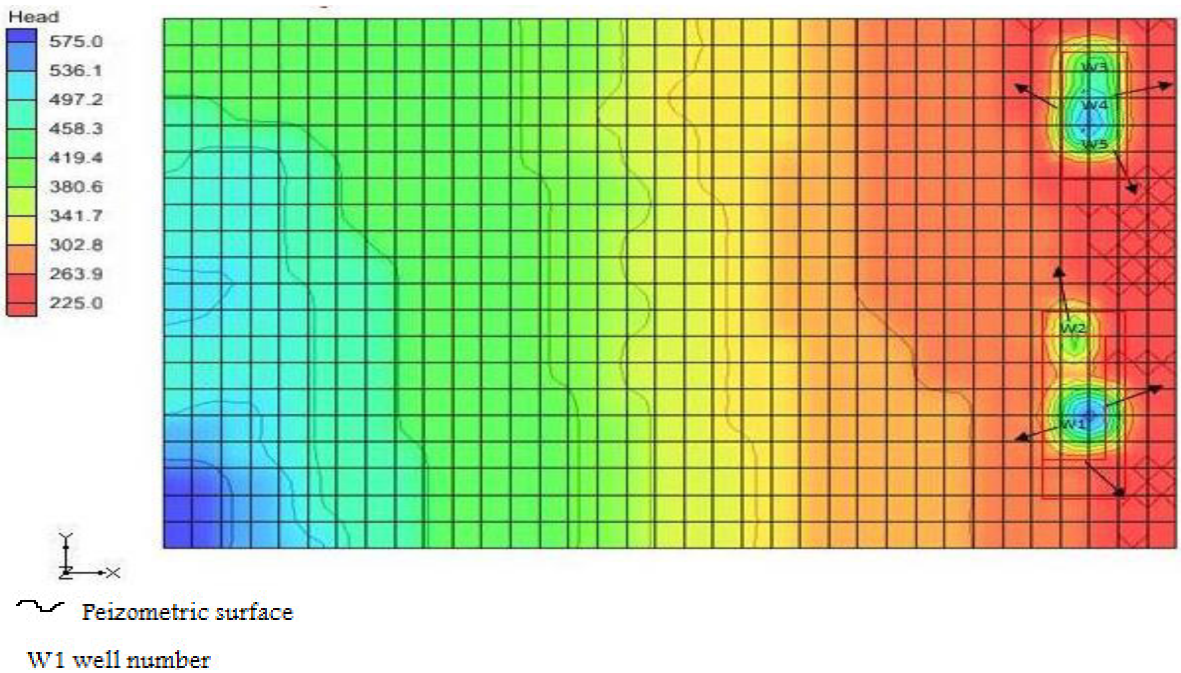

Figure 7. Horizontal cross-section view of the map showing groundwater drawdown from the wells w1, w2, w3, w4 and w5 after the first stress period. Black arrows around the wells showing pumping of wells.

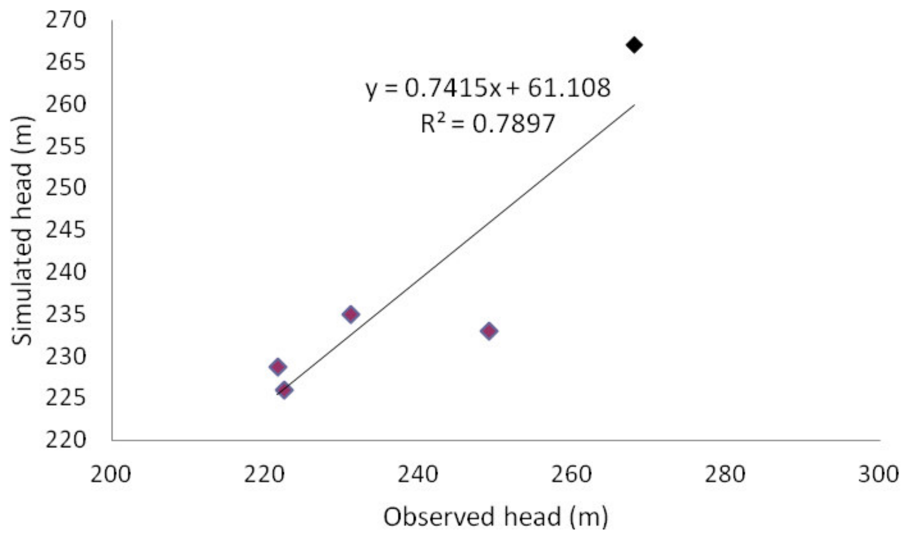

Figure 8. The simulated head and observed head (in meters) for 5 wells in the study area.

The yearly water demand for agriculture shown in Figure 9 suggests that the demand for water for irrigation increases during summers due to high evapotranspiration from the crop. Two irrigation periods were considered for agriculture. The first month begins in February and ends in May, and the other begins in July and ends in September. These are the months where the groundwater demand is more for irrigation purpose because the crops reaches their development stage as shown in Figure 9. Since irrigation also depends on the surface water diversion through CVP, the excess irrigation water percolated to the groundwater table causing water table to rise temporarily during orchards growing season. Orchards are harvested in the month of October. The demand for water also reduces comparatively during post harvest where the irrigation is minimum as shown in the Figure 9. It is understood that water table fluctuate throughout the year depending on the rainfall. However, due to change in climate, lack of rainfall and persistent drought that resulted in high water demand for agriculture. The excess and unregulated irrigation scheduling and management caused percolation of excess water, thus increasing the water table during summer. From the last decade, the groundwater level increased during irrigation months because of its dependency on CVP water allocation and surface water diversions when compared to non-existence of canal system before 1950. As illustrated in Figure 10, the average water surface elevation (WSE) in 1950 for the growing season (May to July) is 161.04 m when compared with 2009, 2010, and 2011 are 237.14 m, 236.28 m, and 235.74 m respectively.

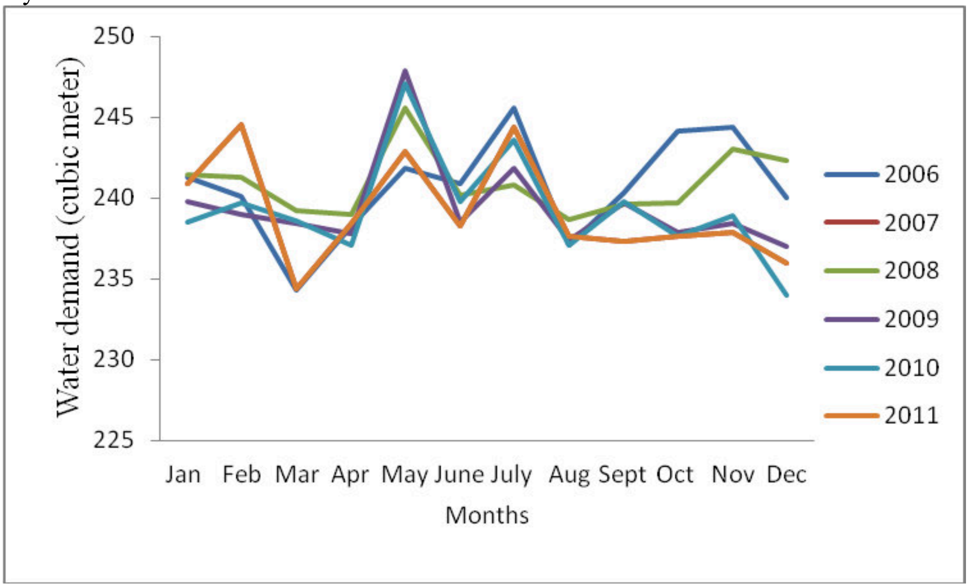

Figure 9. Yearly groundwater demand for irrigation from 2006 through 2012
Data Source: California Department of Water Resources, 2009

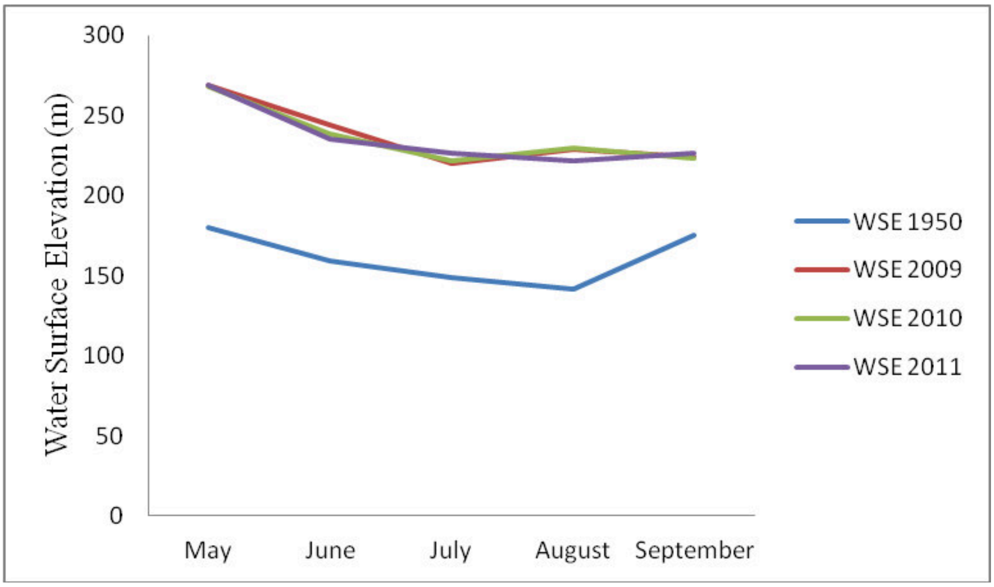

Figure 10. A comparison between the groundwater level between 1950 with 2009, 2010 and 2011. Data Source: California Department of Water Resources, 2009

4. Conclusion

San Joaquin Valley is characterized by frequent droughts for the last few years. The drought in California has direct impact on crop revenue losses of $900 million. In addition, the drought resulted in job loss of 17000 in agricultural sector (The Sacramento Bee, 2016). Revenue from crop increased drastically from $20 billion to $38 billion since 2000. As a consequence of economic factor, farms have adapted efficient water management and irrigation practices such as drip irrigation or changing the crop type to less water-demand crop. California agriculture and irrigation schedule are changing depending upon the water availability to withstand the drought. Indiscriminate exploitation of groundwater for agriculture has adversely affected the availability of groundwater. Groundwater is extracted heavily for irrigation in Tulare, Kern and Fresno Counties during drought years when the surface water delivaries are limited. However, the abstraction of groundwater exceeds the recharge rate. This resulted in decline of groundwater levels throughout California. In this study, we have gathered various inputs from the aquifer parameters and aquifer stresses to construct a mathematical model to simulate the groundwater flow. The model was constructed and validated against the observed water level data for five wells. It was observed that the demand of groundwater increases for the growing season in summer months in the farm. The simulation shows that the irrigated water mostly percolated from the recharge area and moved towards the California Aqueduct. Also, in this study, we compare the ground water level from 1950 to 2009, 2010 and 2011 from the data available in California Department of Water Resources (2009). Since the introduction of Friant - Kern Canal between 1950 to 1955, it is observed that the average water surface elevation (WSE) in 1950 for the growing season (May to July) is 161.04 m. This value is low when compared to those of 2009, 2010, and 2011, which are 237.14, 236.28, and 235.74 m respectively. It is understood that the average water surface elevation increased from the dependency of surface water deliveries and irrigation-water recharge from the farm. This study help to contribute the local farmer and water managers to evaluate the capture zone for potential recharge and analyze the ground water flow direction in the aquifer system at the farm-level in order to understand the agricultural water management. In future studies, an artificial barrier at the capture zone of recharge at farm-level can be useful for tardy movement of water in the sub-surface to groundwater table. This will help the water table to rise during growing season of crop.

References

Bazeley, W.M. San Emigdio Nose oil field. *A.A.P.G. (*1972). *Mem*., No. 16, pp 313-17

Bertoldi, G.L., R. H. Johnston, and K.D. Evenson (1991). Ground Water in the Central Valley, California - A Summary Report 1401-A, *U.S. Department of the Interior, Geological Survey.*

Berry F, Duke Ophori, Jeffrey Hoffman, Robert Canace (2009). Groundwater flow and capture zone analysis of the Central Passaic River Basin, New Jersey. *Environ Geol* Vol. 56, pp. 1593–1603.

Burow, K.R., Shelton, J.L., Hevesi, J.A., and Weissmann, G.S. (2004). Hydrogeologic characterization of the Modesto area, San Joaquin Valley, California: *U.S. Geological Survey Scientific Investigations Report.* Report –5232, pp. 62

Available at http://pubs.usgs.gov/sir/2004/5232/sir_2004-5232.pdf

California Dept. of Food and Agriculture. (2009) http://www.cdfa.ca.gov/egov/Press_Releases/Press_Release.asp?PRnum=09-009

California Department of Water Resources Revised (2009).

Davis, G.H., Green, J.H., Olmsted, F.H., and Brown, D.W. (1959). Ground-water conditions and storage capacity in the San Joaquin Valley, California: U.S. Geological Survey. *Water-Supply Paper*. Vol. 1469, pp. 287.

Faunt, C.C., Belitz, Kenneth and Hanson, R.T. Chapter B. (2009). Groundwater availability in California's Central Valley, in C.C. Faunt, ed., Groundwater availability of the Central Valley Aquifer, California: *U.S. Geological Survey Professional Paper 1766*. Available at http://pubs.usgs.gov/pp/1766/.

Gronberg, J.M., Dubrovsky, N.M., Kratzer, C.R., Domagalski, J.L., Brown, L.R., and Burow, K.R. (1998). Environmental setting of the San Joaquin-Tulare Basins, California: *U.S. Geological Survey Water-Resources Investigations Report 97–4205,* pp. 45

Maupin, M.A., and Barber, N.L. (2005) Estimated withdrawals from principal aquifers in the United States, 2000: *U.S. Geological Survey Circular.* 1279, pp. 46.

Available at http://pubs.usgs.gov/circ/2005/1279/.

Mendenhall, W.C., Dole, R.B., and Stabler, Herman. (1916). Ground water in San Joaquin Valley, California: *U.S. Geological Survey Water-Supply Paper Vol. 398*. pp. 310.

McDonald M.G., and A.W. Harbaugh. (1998). A modular three-dimensional finite-difference ground-water flow model. Techniques of Water-Resources. *Investigations, Book 6. U.S. Geological Survey.*

McDonald M.G., and A.W. Harbaugh (1996a). User's documentation for MODFLOW-96, an update to the U.S. Geological Survey modular finite-difference ground-water flow model. *Open-File Report 96-485. U.S. Geological Survey*.

McDonald M.G., and A.W. Harbaugh (1996a). Programmer's documentation for MODFLOW-96, an update to the U.S. Geological Survey modular finite-difference ground-water flow model. *Open-File Report 96-486. U. S Geological Survey.*

Ophori, D.U., and J. Toth (1989). Characterization of Groundwater Flow by Field Mapping and Numerical Simulation, Ross Creek Basin, Alberta, Canada. Groundwater. Vol 25, No. 2, pp 193-201.

Ratliff L.F., J.T. Ritchie, D.K. Cassel (1983). Field-measured limits of soil water availablility as related to laboratory-measured properties. *Soil Science Society of America*, Vol. 47(770), pp. 5.

Roy, Sagarika, D. Ophori, and S. Kefauver (2013). Estimation of actual evapotranspiration using surface energy balance algorithms for land model: a case study in San Joaquin Valley, California. *Journal of Environmental Hydrology*. Vol. 21, Paper 14

Roy, Sagarika and D. Ophori (2012). Assessment of Water Balance of the semi-arid region in Southern San Joaquin Valley California using Thornthwaite and Mather's model. Journal of Environmental Hydrology. Vol 20, paper 15.

U.S. Bureau of Reclamation (2009). San Joaquin River Restoration Program Programmatic EIS/EIR. Available online: http://www.usbr.gov/mp/nepa/nepa_projdetails.cfm?Project_ID=2940 (Accessed on 7 July 2016)

Williamson, A.K., Prudic, D.E., and Swain, L.A., (1989). Ground-water flow in the Central Valley, California *U.S. Geological Survey Professional Paper* 1401–D, pp. 127.

Webb, G.W. (1977) Stevens and earlier Miocence turbidite sands, San Joaquin Valley, California in guidebook: Late Miocenegeology and new oil fields of Southern San Joaquin Valley, Pacific sections, *A.A.P.G., SEC., S.E.P.M* .

Water and Drought. The Sacramento Bee. Available online: http://www.sacbee.com/news/state/california/water-and drought/article31396805.html (Accessed on 7 July 2016).